

Open camera or QR reader and
scan code to access this article
and other resources online.



A Computational Approach to Explaining Bioelectrically Induced Persistent, Stochastic Changes of Axial Polarity in Planarian Regeneration

Joel Grodstein, MS¹ and Michael Levin, PhD^{2,3}

Abstract

Morphogenesis results when cells cooperate to construct a specific anatomical structure. The behavior of such cell swarms exhibits not only robustness but also plasticity with respect to what specific anatomies will be built. Important aspects of evolutionary biology, regenerative medicine, and cancer are impacted by the algorithms by which instructive information guides invariant or stochastic outcomes of such collective activity. Planarian flatworms are an important model system in this field, as flatworms reliably regenerate a primary body axis after diverse kinds of injury. Importantly, the number of heads to which they regenerate is not determined genetically: lines of worms can be produced, which, with no further manipulation, regenerate as two-headed (2H) worms, or as “Cryptic” worms. When cut into pieces, Cryptic worms produce one-headed (1H) and 2H regenerates stochastically. Neural and bioelectric mechanisms have been proposed to explain aspects of the regenerative dataset. However, these models have not been unified and do not explain all of the Cryptic worm data. In this study, we propose a model in which two separate systems (a bioelectric circuit and a neural polarity mechanism) compete to determine the anatomical structure of a regenerate. We show how our model accounts for existing data and provides a consistent synthesis of mechanisms that explain both the robustness of planarian regeneration and its remarkable re-writability toward novel stable and stochastic anatomical states.

Keywords: developmental bioelectricity, regeneration, planaria, ion channel, gap junction, morphogenesis, resting potential, voltage

Introduction

MORPHOGENESIS IS ONE of the major grand mysteries of biology. While substantial progress is being made on the mapping between genomic information and the micro-scale protein hardware available to cells, significant knowledge gaps remain about the design principles that enable cellular collectives to reliably construct complex, invariant anatomies. Especially critical is understanding not only the molecular genetic pathways that drive emergent morphogenesis but also the signaling dynamics that implement plasticity and adaptive change of large-scale shape. Regulative development, remodeling, and regeneration illustrate

the competence of cellular swarms in solving problems in anatomical morphospace: these swarms are able to work toward specific outcomes and cease growth and remodeling when structures are complete.

Some of the most interesting aspects of this field concern the roles of physical forces (such as biomechanics^{1,2} and bioelectricity^{3–5}) in this process, and the possibility that these modalities enable tissue-level outcomes different from that of the species-specific default in the absence of genomic changes. A number of discoveries about the plasticity of anatomical homeostasis, and the origin of instructive information that guides the activity of cellular collectives, have been made in the free-living flatworm known as the planarian.^{6,7}

¹Department of Electrical and Computer Engineering, Tufts University, Medford, Massachusetts, USA.

²Allen Discovery Center at Tufts University, Medford, Massachusetts, USA.

³Wyss Institute for Biologically Inspired Engineering at Harvard University, Boston, Massachusetts, USA.

Planaria are masters of regeneration; when a planarian is cut into fragments, each individual fragment is capable of regrowing into a fully functional entire worm.^{8,9} Progress is being made on how planarian gradients of position-control-gene expression drive the creation of new shape,¹⁰ regenerating complex organs in the correct bodily position. However, the question of how those gradients re-form, when a planarian fragment regenerates, still remains. In the anterior-posterior axis, a regenerating planarian must determine which end will be the head and which will be the tail. This process is highly reliable, but can go awry in very interesting ways that shed light on how cellular collectives cooperate toward diverse large-scale outcomes. In this article, we unify existing models and propose a new picture of the processes that determine the primary axis of planaria.

There is no shortage of data points for an axial-polarity theory to explain. First, segments of planaria—even small segments from the mid-body—always regenerate their head and tail on the same sides as the original.^{8,9} If we consider a single cut made in mid-body and thus dividing the worm into two separate pieces, then the tissue anterior to the cut (being the rearmost portion of the front piece) will regenerate as a tail, while the tissue just posterior of the cut (being the frontmost portion of the rear piece) will regenerate as a head. Since before the cut both tissue fragments were adjacent and shared the same local morphogen concentrations, clearly long-range communication is required for cells to solve this problem.

Evolution discovered long ago (at about the time of bacterial biofilms^{11,12}) that electrical networks are excellent ways to propagate information long range and make decisions about large-scale system-level behaviors. Before their use in neural circuits to drive muscle motion, developmental bioelectricity enabled decision-making, such as organ identity, size, axial polarity, and shape, in non-neural tissues during morphogenesis.^{13–15} Bioelectricity has been shown to coordinate collective cell decisions during patterning of the left-right axis,^{16–19} craniofacial development,²⁰ and long-range influences on brain patterning^{21–23} and carcinogenic transformation.^{24–26}

In prior work, we had explored the hypothesis that bioelectric signaling, through electrical synapses known as gap junctions (GJs),²⁷ underlies the ability of planarian wounds to decide whether to make heads or tails, by enabling them to integrate local states with those of distant tissues.^{28,29} Loss-of-function experiments with GJs^{30,31} and ion channels^{32,33} revealed that indeed this system was critical in the normal determination of head-tail polarity, and double-head or no-head worms were readily produced by interfering with bioelectrical signaling immediately after amputation. However, many questions still remain about the logic and mechanisms by which bioelectric circuits control anatomical outcomes in planaria.²⁸

There is a notable head-to-tail V_{mem} gradient in planaria, with the head at a higher (i.e., more depolarized) V_{mem} than the tail,^{32,34} presumably resulting in an internal electric field. It is thus somewhat unsurprising that one of the earliest experimental data points on axial polarity is purely electrical.

Even though segments of planaria in the wild always regenerate their head and tail on the same sides as the original, application of a strong electrical field during regeneration, appropriately polarized in opposition to the internal

field, reverses this. Furthermore, application of a somewhat weaker electrical field (intuitively, strong enough to cancel, but not reverse the internal field) results in a two-headed (2H) regenerate.^{8,35,36} Finally, directly altering V_{mem} at the head and tail with ion-channel drugs also changes which end generates a head and which a tail.³² These data strongly suggest that an electrically charged morphogen is involved.³⁷

Later experiments³⁰ showed that using octanol to block GJs also resulted in 2H regenerates. Perhaps the most well-known use of GJs is conducting action potentials in mammalian cardiac tissue. However, they also play a role in electrical communication of numerous small molecules.³⁸ The combination of axial-polarity reversal and 2H regenerates by electrical fields, and producing 2H regenerates by blocking GJs, led to the *electrodiffusion* hypothesis of axial polarity.^{39,40}

In this hypothesis, axial polarity is controlled by a charged morphogen M that is a small ion. If it were negatively charged, then an existing head-to-tail V_{mem} gradient would attract M to the head; it would move through GJs to travel between cells. With enough M near the head, the resulting diffusion flux would move it backwards in a manner very similar to the Nernst equation.⁴¹ However, this would not explain how a V_{mem} gradient gets regenerated in a small fragment. The hypothesis thus adds positive feedback; not only does a higher V_{mem} attract M but also a higher $[M]$ gates ion channels to increase V_{mem} . This hypothesis has been well simulated and can be quite robust.^{40,42}

However, the electrodiffusion hypothesis is likely not complete, because the long-known role of neural inputs into polarity during regeneration^{43–45} appears to be conserved in planaria.⁴⁶ As a result, an *axonal transport* hypothesis has been proposed.^{37,47} Neurons are very long cells, and thus move nutrients between organelles actively with axonal transport rather than relying solely on diffusion. The axonal-transport hypothesis proposes that this same mechanism additionally transports a morphogen. The largest mass of neurons in a planarian is the ventral nerve cord (VNC), which predominantly runs from head to tail. Transport from the front of a planarian to the rear, combined with the resulting diffusion back toward the front, would produce a classic morphogen profile.

There is substantial evidence⁴⁸ for the involvement of WNT signaling in creating head-to-tail planarian morphogen gradients, along with numerous gain-of-function and loss-of-function experiments on transcription factors (TFs) involved with WNT. The hypothesis thus proposes a gene regulatory network (GRN) which, when combined with the anterograde transport of Hedgehog and retrograde transport of a proposed Notum Regulation Factor (*NRF*), is consistent with the existing RNA interference (RNAi) data.

The axonal-transport hypothesis is further supported as follows⁴⁷: first, it correctly predicts the results of RNAi experiments on the motor proteins involved in axonal transport. Second, while the planarian VNC runs largely from head to tail, neurons in some other areas run predominantly mediolaterally. New experiments that regenerate fragments cut from these areas consistently produce regenerates whose head-to-tail axis is now rotated 90°—that is, which follow the predominant neuronal direction rather than the direction of the original head-to-tail axis.

While axonal transport is attractive, it does not explain our electrical-manipulation data. Furthermore, it does not specify the mechanism for morphogen transport between neurons, and we will see below that it also cannot explain all of the GJ data. Finally, neither it nor electrodiffusion can explain a final piece of experimental data—Cryptic worms.

Cryptic worms were discovered as a result of a gap-junctional-blockade experiment. As noted above, this typically produces 2H regenerates. However, there were also some seemingly normal, 1H regenerates.

Our previous hypothesis was that the 1H fraction of a cohort exposed to octanol was comprised of “escapees,” indicative of incomplete penetrance of our treatment or some variability in worms’ susceptibility to the reagent. However, it was observed that when amputated in plain water, such animals maintain roughly the same proportion of 1H:2H resulting regenerates.³⁴ This persists in multiple rounds (generations) of recutting, despite a wild-type (WT) genomic sequence and no further treatments. Thus, rather than 2H’s and WT escapees, what GJ blockade really produces is 2H’s and a permanent line of animals in which the head-determining information is destabilized, fluctuating stochastically upon each cut.

They are called Cryptic because their normal anatomy and gene expression profiles belie a disorder of patterning information that is not readily apparent. The offspring of fragments from such worms, including two lateral pieces cut from the same anterior-posterior position of a single Cryptic worm, make independent decisions about whether they will be 2H or Cryptic (one head, but destabilized). The models that have been proposed to explain persistent bioelectric memory of one versus two head decisions, and Cryptic worms’ destabilized morphology, have never been unified into a single framework to understand how head number is determined by physiological signaling.

In summary,

- The axonal-transport hypothesis⁴⁷ specifically chose its associated GRN so as to explain numerous loss-of-function experiments on regulatory TFs. It explains those data quite well. Furthermore, it correctly predicts new results for loss-of-function experiments on the motor proteins involved in axonal transport as well as various new cutting scenarios.
- The electrodiffusion hypothesis explains various experiments that involve applied electrical fields, as well as experiments involving GJ blockers and interventions targeting cell V_{mem} (e.g., hyperpolarization or depolarization).
- Neither hypothesis explains the opposite set of experiments. This is unsurprising—the axonal-transport hypothesis does not have V_{mem} or GJs as an input and thus cannot explain electrical or GJ effects. Similarly, the electrodiffusion hypothesis does not make any use of any of the TFs in the loss-of-function experiments.
- Neither hypothesis seems capable of proposing a mechanism for Cryptic worms.³⁴

In this study, we propose a hybrid model that explains essentially all the above data points. It also explains Cryptic worms quite simply. There are numerous data points to explain, which our new model addresses:

- The ability of planarian head-tail axes to regenerate reliably from small fragments.
- The effect of an applied electric field to create a 2H regenerate, or a larger field to reverse head-tail polarity.^{35,36}
- Data from Oviedo et al.³⁰ shown in Figure 1. It includes various cuttings, with and without octanol.
- Data from Bischof et al.⁴⁶ showing how the gradually changing planar-cell polarity in a 2H worm correlates with which cuttings regenerate as 2H (Fig. 2).

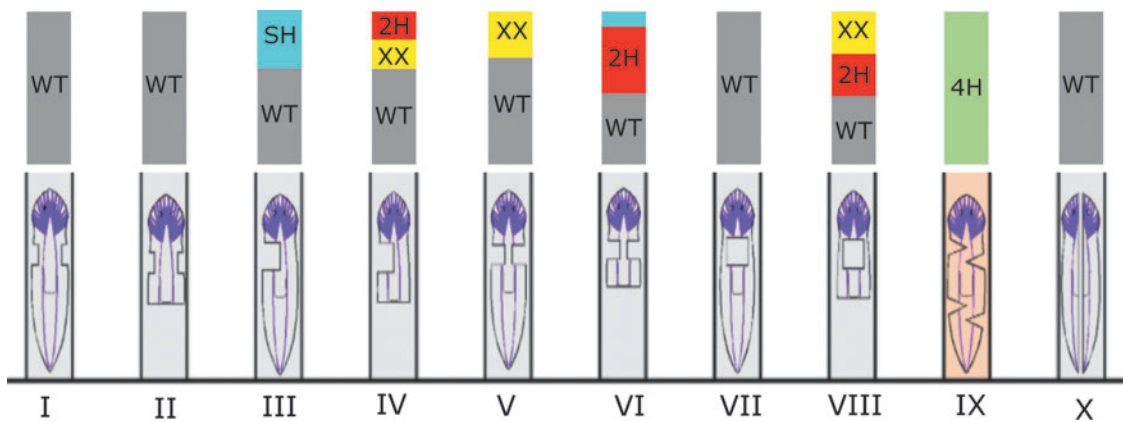


FIG. 1. Summary of experiments from Oviedo et al.³⁰ This figure is a simplified version of Oviedo et al., figure 1C (see the original for full detail). It summarizes the numerous planarian cutting experiments, cutting and notching worms in different locations relative to the VNC. The graphs are shown with the size of each color proportional to the frequency of the corresponding phenotype. E.g., case III has 65% wild-type and 35% side-head. Graph legend: WT, wild type (grey); 2H, two-headed (red); 4H, four-headed (green); SH, side-head (blue); XX, other (yellow). All cases I–X in fresh water with no octanol resulted in WT outcomes. A VNC-only theory cannot easily explain that, but adding V_{mem} control makes it easier to explain these results. Consider the notches—when regenerating in water, the notches only slightly disturb the existing V_{mem} pattern, with the result that regeneration works correctly. Even when cutting the VNC, the correct V_{mem} pattern is instructive enough to the GRN that we get correct regeneration. However, octanol allows V_{mem} islands and breaks the V_{mem} reference, yielding improper regrowth. The combination of impairing the V_{mem} system with various forms of breaking the VNC system yields unusual results, including a wide variety of “other” cases. 2H, two headed; GRN, gene regulatory network; VNC, ventral nerve cord; WT, wild type.

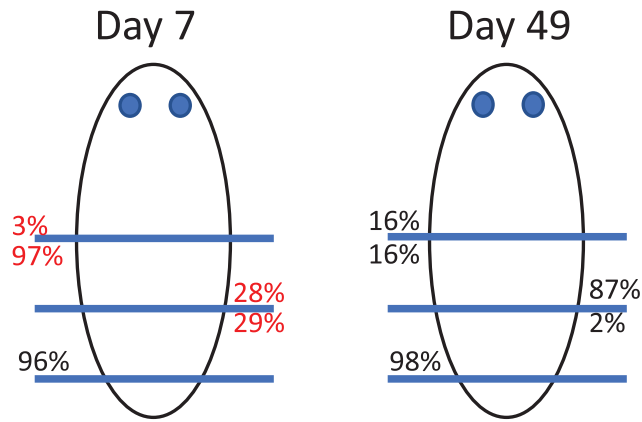


FIG. 2. Summary of experiments from Bischof et al.⁴⁶ This figure is condensed from Bischof et al.,⁴⁶ figure 4, and summarizes their experiments cutting and regenerating 2H worms. Start with a 2H worm. Cut it at one of three cut lines shown, leaving a front-of-cut and a rear-of-cut fragment. The two numbers at each cut line are the percent of 2H worms that regrew as 2H for the given fragment on the given day. Numbers most inconsistent with an electrodiffusion-only model are in red. The most obvious way to fix this inconsistency is to assume substantial “tail pressure”—that is, that the VNC tail pushes V_{mem} more negative. Thus, the V_{mem} profile would roughly match the VNC-polarity profile.

- Data on Cryptic worms from Durant et al.³⁴ (Fig. 3).
- An unusual 90° rotation of the head-tail axis in Pietak et al.⁴⁷ (Fig. 4).
- All the RNAi loss-of-function data mentioned in Pietak et al.⁴⁷

Results

A simple extension of the axonal-transport hypothesis still does not explain all the data

Many interventions in the literature that produce altered phenotypes involve octanol, a GJ blocker (Figs. 1 and 3). However, neither octanol nor GJs play any part in the axonal-transport hypothesis, which thus does not explain octanol’s results.

We will propose a hybrid hypothesis, including polarity control not only by the VNC but also by electrodiffusion through GJs. Is this unnecessarily complex? Could we perhaps simply extend the axonal-transport hypothesis to include GJs and thus not need electrodiffusion?

One might merely assume that the VNC neurons communicate through GJs. There is substantial precedence for this; the mammalian heart is dominated by excitable tissue (cardiomyocytes) that predominantly communicates through GJs. Furthermore, many neurons in the central nervous system communicate through GJs rather than chemical synapses^{49–51} and myocytes are known to express position-control genes.¹⁰ Thus, it may be reasonable to assume that the length of the planarian VNC spans multiple neurons, and that those neurons interconnect through GJs. On this hypothesis, GJs could be part of the VNC and thus octanol would affect VNC functioning. Does this avoid the need to use electrodiffusion at all?

Unfortunately, this simpler hypothesis does not fit the data. Figure 1 is adapted from figure 1C of Oviedo et al.³⁰ It shows that cutting the VNC alone is not sufficient to produce altered phenotypes; all cases in Figure 1 regenerated correctly in water, even with the VNC cut. Furthermore, Figure 1 cases I, II, and X show that blocking GJs with octanol is not sufficient

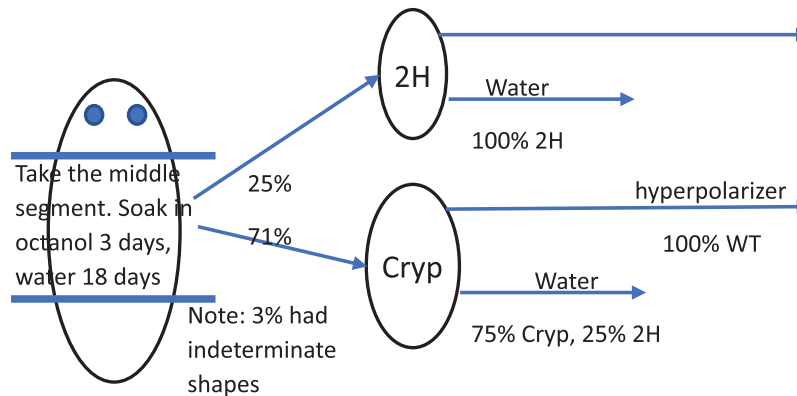


FIG. 3. Summary of Cryptic-worm experiments. This figure summarizes the Cryptic-worm experiments from Durant et al.³⁴ The original WT worms are on the left, which then undergo a 3-day octanol treatment to temporarily disrupt GJs. This results in some 2H regenerates, with the remaining being Cryptic. The Cryptics, upon recutting in fresh water, show the same stochastic regeneration as our WT showed when exposed to octanol. Why would not octanol produce, for example, HTHTHT? Because even though the octanol reduces GJ conductance enough for such patterns to occur, they vanish as soon as the octanol is removed. Why do not we ever get THT? A reasonably high head pressure and low tail pressure would explain that—the head pressure would force the VNC head to remain a head (and outlaw THT). The low tail pressure would allow the VNC tail to become depolarized. Of course, some worms will have HTHTHT flatten to just TH, but that’s fine. A VNC-only theory cannot explain how WT+octanol could ever produce 2H, since both VNCs remain intact and octanol is not part of the GRN from ref. 47. We easily explain hyperpolarizing a Cryptic. The hyperpolarizer pulls V_{mem} negative everywhere. As soon as the hyperpolarizer is removed, VNC head and tail pressure will depolarize the head and keep the tail hyperpolarized—reliably giving a WT V_{mem} profile. A similar argument explains hyperpolarizing a 2H. VNC head pressure at both ends will tend to give us a 2H V_{mem} profile rather than WT—and we indeed see only 1/3 of 2H convert to WT. Perhaps the occasional conversion to WT in the data happens since having both heads swing from fully hyperpolarized to fully depolarized may be enough dynamic movement to occasionally swing the V_{mem} system into a WT profile (which is, after all, fully stable). GJs, gap junctions.

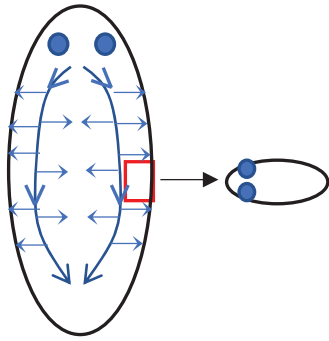


FIG. 4. Summary of the 90° rotation from Pietak et al.⁴⁷ Summarized from Pietak et al.⁴⁷ Planarian fragments in previous work typically regenerate either as WT or with some version of head and tail in the anterior or posterior end of the worm. This experiment showed an unusual 90° rotation. Although the planarian VNC runs from head to tail, portions of its nervous system naturally run side-to-side in certain areas of the worm (as shown). This experiment took a fragment specifically from one such location; the result is a new worm rotated by 90°. This is exactly what a VNC-based hypothesis would predict.

to produce altered phenotypes unless the VNC is cut. That is, neither cutting the VNC alone nor octanol soaking alone hindered normal regeneration. Instead, breaking the regenerative process required *both* interventions simultaneously. If morphogenetic cues were truly propagated through GJ-connected neurons in the VNC, then *either* of two interventions would have been sufficient to disrupt the system.

Having VNC neurons communicate through GJs places axonal transport in series with GJs and would require both to function. We must thus reject this attractively simple hypothesis—our hybrid hypothesis instead places electrodiffusion in *parallel* with axonal transport, thus only requiring one of the two to function and better matching the data.

A new, hybrid hypothesis

We start by hypothesizing that *both* models discussed above—electrodiffusion and axonal transport—exist. Furthermore, they affect each other through cross-coupling:

- The VNC influences the electrodiffusion system through *head pressure* and *tail pressure*. Specifically, axonal transport is known to create a gradient of various TFs. We hypothesize that one or more of these TFs then leaves the VNC and (directly or indirectly) gates ion channels so as to hyperpolarize numerous non-neural cells at the worm's tail and depolarize non-neural cells at the head.
- The GRN from Pietak et al.⁴⁷ does not have any electrical input. We add it—namely, we hypothesize that V_{mem} modulates (directly or indirectly) the activity of one or more TFs in the GRN.
- This cross-coupling allows each system to influence the other, and hence allows both systems to influence the final regenerative outcome (Fig. 5).

We do not, in this study, specify the molecular level details of the cross-coupling. However, there are numerous mechanisms in nature by which chemical and electrical networks

influence each other.^{14,52} TFs (being proteins) do not typically cross a cell membrane and thus may not be expected to exit the VNC. However, there are exceptions such as Nkx3.1,⁵³ Pax6,⁵⁴ and OTX2, which are secreted from neurons and transported within embryos.^{55–59} Moreover, neurons are capable of modulating nearby cells through neurotransmitters, GJs, and repurposed retrotransposons like ARC.^{60,61}

A hybrid system can explain Cryptic worms

The key claim in the hybrid hypothesis is that two systems coexist: axonal transport through the VNC and electrodiffusion through GJs. Each system is quite robust, and so under normal circumstances, they each tend to stabilize at a state that induces a normal WT phenotype—which means the two systems are aligned with each other. When one system, due to occasional unreliability, drifts toward an unnatural phenotype, the cross-coupling helps to bring it back.

We hypothesize not only that both systems exist but also that their state is different in Cryptics. We propose that the destabilized property of Cryptic worms arises because two components of the anterior-posterior axis-determining system are out of alignment with each other, leading to conflicting signals and competing forces within the cellular collective. Durant et al.³⁴ showed (their fig. 3) that a Cryptic worm's VNC is still WT. They also used DiBAC staining^{62,63} to measure a Cryptic worm's V_{mem} profile to be 2H.

The resolution of DiBAC staining leaves much to be desired; improvements in voltage imaging *in vivo* will be necessary to acquire more definitive, high-resolution V_{mem} profiles for all the conditions discussed herein (as well as for deeper tissues that have not yet been accessible to this technology). Thus, for the purposes of this model, we will assume that Cryptics have the same 2H V_{mem} profile as in Durant et al.³⁴

Even though the cross-coupling is strong enough to keep the two systems aligned in nature, it is not strong enough to guarantee alignment under chemical interventions such as octanol. We propose that Cryptic worms represent the combination of a 2H electrodiffusion state with a WT VNC state. However, how exactly could octanol generate this mismatched state?

Grodstein and Levin⁴² showed that an electrodiffusion model predicts that decreasing GJ connectivity naturally induces multiple swings between hyperpolarized and depolarized (Fig. 6), essentially dividing the worm into *voltage islands* (as also shown experimentally in Emmons-Bell et al.⁶⁴). Octanol is a GJ blocker—its main effect is precisely to decrease GJ connectivity.^{65,66} Thus, octanol will induce exactly these multipolar (e.g., HTHHT) V_{mem} patterns. The protocol used to create Cryptic worms starts with an octanol soaking of freshly cut planaria fragments, but then removes the fragments from octanol and places them into fresh water.

This method produces the previously described mixture of 2H animals and animals that look normal (one headed), but are really Cryptic, that is, that they have a destabilized, stochastic propensity to form Cryptics or 2H animals in subsequent cuts.³⁴ As the octanol in the worm is gradually replaced by water, the number of voltage islands will naturally diminish. If the V_{mem} pattern started as, for example, HTHHT, it should naturally swing through HTHHT and then HTH.

As noted above, DiBAC is an imprecise technique due to limitations of depth penetration into the opaque worm, the

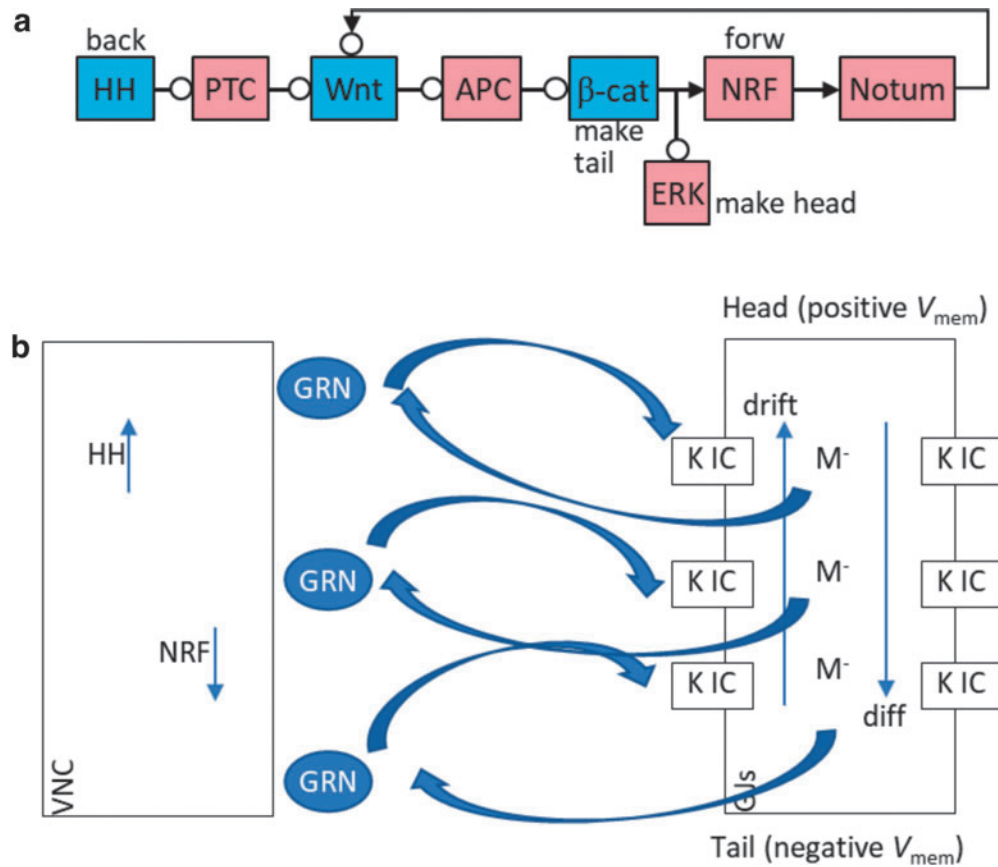


FIG. 5. Pictorial of our hybrid hypothesis. **(a)** Our hypothesis starts with the axonal-transport system from Pietak et al.⁴⁷ *HH* and a hypothesized *NRF* are transported in an anterior and posterior direction, respectively, and diffuse back, creating gradients. Those gradients affect a GRN (with copies in each cell), which then drives creation of a head or tail. The other components of the GRN are *Wnt*, *APC*, β -catenine, *Notum*, and *ERK*. **(b)** The GRN from **(a)** is instantiated in multiple cells on the left of the figure. Electrodiffusion through GJs is shown on the right (vertical blue arrows). It is drawn for simplicity as long arrows; in reality, it is many cells connected by GJs. The negatively charged morphogen *M* moves anteriorly from drift and then diffuses posteriorly. Its concentration then affects ligand-gated ion channels (for potassium in our model), which in turn affect V_{mem} and drive the drift currents. The left-to-right curved arrows show one cross-coupling between the two systems, with the VNC providing *head and tail pressure* onto V_{mem} by affecting K ion channels. The right-to-left curved arrows show the other cross-coupling, with V_{mem} as a new input into the GRN. *APC*, adenomatosis polyposis coli; *ERK*, extracellular regulated receptor kinase; *HH*, Hedgehog; *NRF*, Notum Regulation Factor.

almost incessant movement of planaria, and the difficulty of calibrating dye signal to absolute V_{mem} electrophysiology; thus, we cannot claim to know the exact shape of the V_{mem} profile. However, that is largely irrelevant to our hypothesis—we require only that the head region(s) are depolarized relative to the body regions, and that making GJs less conductive makes it easier for regions of hyperpolarization and depolarization to exist in close physical proximity.

We assume that default GJ connectivity without octanol is such that an HTH V_{mem} state is stable. Thus, worms do not *pass through* HTH on the way to TH (i.e., to a WT V_{mem} profile), but instead stay at the stable HTH pattern, which corresponds to a 2H phenotype. Thus, the temporary octanol intervention tends to result in electrodiffusion, reaching a stable 2H state. However, there has been no intervention in the VNC, so the axonal-transport GRN naturally tends to remain in a WT state.

In roughly 1/3 of worms (where again the precise number can vary in this stochastic phenotype), the cross-coupling is

strong enough that the 2H electrodiffusion state pushes the VNC GRN into a 2H state and we get a true 2H phenotype. However, in the remaining roughly 2/3 of worms, we propose that cross-coupling is not strong enough to flip the VNC-GRN state, thus resulting in a new phenotype—electrodiffusion in a 2H state and the VNC in a WT state. We posit that this is a Cryptic worm. What might cause this stochasticity? Chemical reactions are governed by statistical mechanics; while macroscopic systems are typically quite deterministic, cells are small and thus have an inherently high noise level.⁶⁷ When two systems influence each other through metabolite amounts and reaction rates that are not fully predictable, stochasticity naturally occurs.

Durant et al.³⁴ showed that Cryptics exhibit stochastic regeneration up to 8 weeks after their initial cutting. Thus, if we accept that the discordance between a Cryptic worm's electrical state and its VNC state is the source of the stochasticity, then this discordance is long lived. That is, in the Cryptic state, both systems are not only stable but also can remain so despite disagreeing with each other—the cross-

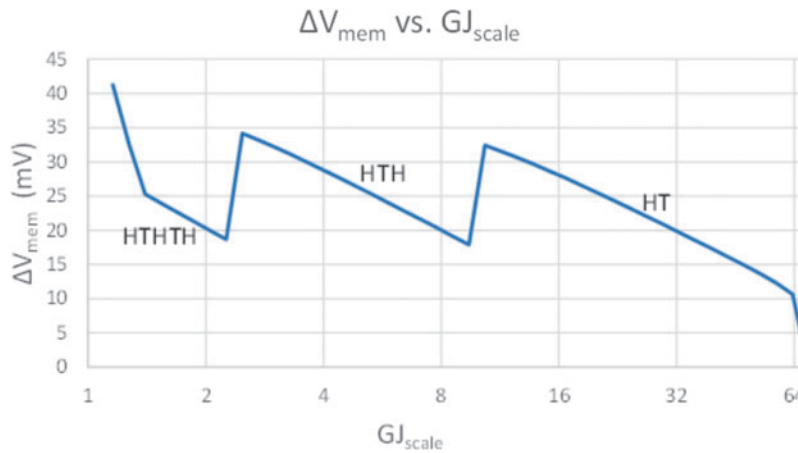


FIG. 6. Swings in V_{mem} as GJ_{scale} changes. This picture is repurposed from figure 1 of Grodstein and Levin.⁴² Here, it shows how a 2H electrical system can be the natural result of a temporary octanol bath. The x axis represents GJ_{scale} (i.e., the density of GJs relative to an arbitrary reference); the y axis is ΔV_{mem} (the delta between the highest and lowest V_{mem} anywhere in the worm). Each portion of the graph is also labeled with the worm's overall pattern of heads and tails, as read from peaks and valleys of V_{mem} distribution across the worm. A worm with octanol starts on the left side of the graph (very low GJ connectivity). The “HTH” label indicates that V_{mem} may range from depolarized (typical of a head, or “H”) to hyperpolarized (typical of a tail, or “T”) and swinging up and down with a three-headed, two-tailed overall V_{mem} pattern. This is indicative of five voltage islands. As the octanol is washed away, we move rightwards on the graph (i.e., increased GJ conductivity). This forces nearby cells to have more nearly the same V_{mem} ; the number of voltage islands diminishes and the V_{mem} pattern drops to HTH (i.e., a 2H worm), and then HT (i.e., wild type). We claim that the default GJ density is on the range [2.5,9] on this graph, which allows HTH to be stable. Graph taken from Grodstein and Levin.⁴²

coupling between the systems is not strong enough to immediately force them into agreement, as revealed in the fact that stable Cryptic worms exist. However, each regeneration is a statistical opportunity for the cross-coupling to bring the two systems into agreement. Once the two systems are consistent in any worm, future regeneration is no longer stochastic.

This explains Cryptic regeneration in fresh water. With electrodiffusion already in a 2H state, we have no need of octanol to create the 2H state. However, the cross-coupling mechanism between V_{mem} and the GRN still functions identically, resulting in the same roughly 1/3-to-2/3 ratio of 2H and Cryptic regenerates as before, which will continue indefinitely across generations.

Durant et al.³⁴ used hyperpolarization to “revert” Cryptics back to having only one head. After hyperpolarization, Cryptic worms become WT, and thereafter never regenerate in fresh water as 2H. The hybrid hypothesis explains these data easily. Hyperpolarization of the worm brings all cells to nearly the same V_{mem} , thus mostly wiping clean the original 2H V_{mem} distribution. However, the VNC GRN in a Cryptic is still WT. Thus, as V_{mem} regenerates, coupling from the GRN will naturally push V_{mem} into a WT pattern, which is exactly what data from Durant et al.³⁴ show.

We have shown how a hybrid theory naturally explains Cryptic worms, which have been one of the most puzzling aspects of planarian regeneration. We next show how the hybrid theory explains various other pieces of data, one by one.

A hybrid theory explains numerous RNAi interventions as well as 90° body rotation

Pietak et al.⁴⁷ do a very effective job proposing a GRN that predicts the data from numerous loss-of-function experiments. The hybrid theory assumes that this GRN is correct

(although missing an input from V_{mem}), and that axonal transport feeds into it exactly as in Pietak et al.⁴⁷ The hybrid theory thus explains all the loss-of-function experiments that Pietak et al.⁴⁷ do. Since none of these experiments targeted altering cellular V_{mem} , our proposed V_{mem} input into the GRN would not make any difference in the results.

Pietak et al.⁴⁷ also predicted the results of a new type of planaria cutting; a small sideways-directed fragment from the worm's side (Fig. 4), which produced a worm oriented at 90° to the original A-P axis. Our hybrid theory explains this by noting that the geometry of this fragment set up a conflict between the VNC direction (which had a 90° rotation) and the V_{mem} gradient (still in the original direction). In their experiment, the VNC direction reliably won the conflict. However, we predict (see A Hybrid Hypothesis Makes Testable Predictions section below) that by making the fragment longer in the A-P direction, the results could be reversed.

VNC tail pressure can explain regeneration of young 2H worms

Bischof et al.⁴⁶ present data showing the location of a “collision zone” to be a strong predictor of whether newly regenerated 2H planaria regenerate as 2H or as WT. They show the cilia direction to be moving fluid backwards on a WT worm; then, as a newly regenerated worm becomes 2H, the flow direction of the rearmost portion of the worm reverses. The reverse-direction tail segment grows longer over several weeks, until eventually the entire rear half of the worm has reversed cilia direction. They denote the meeting point of the two oppositely polarized worm segments as the collision zone.

Figure 2 recaps their data, collected by cutting a newly formed 2H worm at various time intervals after its initial

regeneration as 2H. It shows that as the “collision zone” moves toward the worm’s center, the likelihood of various worm fragments regenerating as 2H changes accordingly. Essentially, a fragment is much more likely to regenerate as 2H if it includes the collision zone.

Why might cilia direction affect phenotype fate? While their experiments merely measured the direction of cilia flow, one might assume (and indeed we hypothesize) that the gradual change in cilia direction is a marker for a change in VNC direction (an overall linkage to the planar polarity of the tissue^{46,68}). If this is the case, then the model in Pietak et al.⁴⁷ is a simple explanation for Figure 2—Figure 2 shows the head-tail polarity following the cilia direction, which would then be caused by the VNC direction.

A hybrid theory explains these data in two parts. First, as always, we accept the VNC hypothesis and thus accept the statement that a fragment that starts regeneration with a 2H VNC-GRN state will tend to keep that state as it regenerates. However, the most hyperpolarized V_{mem} in a 2H worm naturally occurs somewhere in the worm’s mid-body region.³⁴ Since the early-stage 2H regenerates from Bischof et al.⁴⁶ still had their collision zone near the newly formed head, some fragments, including the middle of the worm, would seemingly have included the V_{mem} minimum, but only included a normal VNC polarity. From our previous discussion, they should have regenerated as Cryptics. However, Bischof et al.⁴⁶ did not observe any Cryptics—why not?

Our hypothesis posits *coupling* from the VNC to V_{mem} , that is, it posits that TFs located at the VNC tail will affect ion channels that result in hyperpolarizing V_{mem} . This will tend to move the location of the most hyperpolarized V_{mem} to near the polarization collision zone. In fact, since we hypothesize that the collision zone is the meeting of *two* VNC tails, we would expect high concentrations of TFs, and this effect will be still more pronounced. We thus expect that the position of the worm’s minimal (i.e., most hyperpolarized) V_{mem} value will move along with the collision-zone location. In other words, worm fragments that include the collision zone will not only start with a 2H VNC state but will also start with a 2H V_{mem} state. For both reasons, they are far more likely to regenerate as 2H than fragments that do not include the collision zone.

A hybrid hypothesis explains the general scheme of regeneration with VNC notches

Figure 1 (taken from Oviedo et al.³⁰ fig. 1C) shows the results of regenerating planaria after numerous interesting cuts. With the VNC notched as shown, all worms successfully regenerated as WT in fresh water. This is challenging to explain with a VNC-only theory; many of the worms have multiple VNC cuts that should have disturbed VNC communication enough to break axonal transport and thus disturb regeneration.

However, it is consistent with our hybrid theory; notching the VNC should not greatly disturb electrodiffusion. The resulting fully normal WT V_{mem} distribution couples into the VNC so as to produce a normal WT phenotype even if the VNC is no longer fully functional. However, when Oviedo et al.³⁰ added octanol, the original WT V_{mem} instead becomes voltage islands. A similar mechanism then occurs as with Cryptic worms; as the octanol is removed, V_{mem} tends toward 2H.

However, in this case, the context is far more complex. Consider, for example, Figure 2 drawing III. At the notch, the left-side VNC is split into two segments. The VNC GRN on the front of the segment below the notch will attempt to regrow a head at the notch’s lower edge, while the VNC segment above the notch will attempt to regrow a tail at the notch’s upper edge. As the notch heals, the various TFs for the two different outcomes will mix diffusively with quite difficult-to-predict results. The cross-coupling between the V_{mem} islands and the VNC will complicate the system still further.

As a result, the precise outcome of most of these experiments becomes challenging for a model to predict; indeed, Oviedo et al.³⁰ reported a statistical mix of numerous phenotypes in some of these cuttings. Note that other VNC cuttings (especially those that remove substantial pieces of flesh and hence disrupt electrodiffusion) do reliably produce phenotypes other than WT even in plain water⁴⁷; it depends on the precise cutting pattern.

A hybrid hypothesis makes testable predictions

The hybrid hypothesis makes new predictions in three different categories. First, more predictions about Cryptic worms:

- We predict that the front half of a Cryptic will *always* regenerate as WT. In the front half of a Cryptic worm, both the electrical and VNC state agree, and both predict a WT worm. We predict that all front halves, after cutting, will regenerate as WT. This should be true whether or not the fragment includes the Cryptic head.
- The rear half of a Cryptic will sometimes spontaneously reverse its head and tail direction. In the rear half of the worm, the VNC state is that of a WT worm, while the electrical state is that of a *reversed* WT worm. We predict that, when the electrical state wins at both ends of the worm, the result will be a WT worm with a flipped A-P axis relative to its parent worm. We also predict that this will only happen when the original tail is removed, since otherwise there will not be a rear blastema.

Second, we make further predictions about the experiments in Bischof et al.⁴⁶ and Pietak et al.⁴⁷:

- Bischof et al.⁴⁶ showed that worm fragments that included the collision zone were more likely to regenerate as 2H than other worms. We suggest that measuring V_{mem} as the collision zone moves will show the location of the V_{mem} minimum moving correspondingly. This is a straightforward prediction from our hybrid theory. It is the result of tail pressure from the VNC collision zone onto V_{mem} .
- Pietak et al.⁴⁷ showed that a sideways cut from a particular worm location regenerates at a 90° angle to the original A-P axis. We predict that a similar, but longer segment would not regenerate sideways. As the fragment gets longer, it will start with a larger V_{mem} gradient, which will eventually overcome the 90° VNC rotation. (Note that this experiment currently presents technical difficulties).

Finally, and perhaps most importantly, we note that existing experiments have involved either RNAi⁴⁷, or disturbances of

GJs or V_{mem} ^{20,33,34}—but never both at once. This is essentially why the two different theories explain a nonintersecting set of data points. We propose combining both electrical and GRN interventions in the same experiment, thus allowing us to localize exactly where the two systems interact. Hyperpolarizers such as SCH-28080 electrically promote 2T worms.³⁴ We can combine this with any GRN intervention that creates 2H worms, such as β -cat RNAi, WNT RNAi; or a cAMP inhibitor.⁴⁷

The electrical intervention will only win if the point where V_{mem} affects the GRN is downstream of the TF, which we have interfered with through RNAi. So if, for example, the GRN intervention wins for β -cat, but the electrical intervention wins for cAMP, we would conclude that V_{mem} is acting on cAMP or on adenomatous polyposis coli (APC; which is the GRN predecessor to cAMP; see Fig. 5).

Ionophores (e.g., nigericin and monensin) act to depolarize cells³³ and thus electrically promote 2H worms. Octanol has a similar effect at the front and rear of the worms, as discussed above. We can combine either of these with various GRN interventions that create 2T worms, such as RNAi of Notum or APC.⁴⁷ Again, the results showing which interventions result in the electrical system winning and which result in the RNAi winning will localize the connections between the two systems.

Classic planarian experiments^{35,36} used an electric field to reverse a worm's anterior-posterior polarity. Since there is no known GRN intervention that produces a reversal of polarity, we can combine these classic experiments with any GRN intervention.

We expect the results of these experiments to not only help localize exactly where the cross-coupling points are but also to provide more data that are explained *only* by the hybrid hypothesis.

Methods

We have tested our hybrid hypothesis computationally through numerous simulations. The electrodiffusion model has various parameters, such as the valence and diffusion rate of the morphogen M , the amount of cross-coupling between the VNC and electrodiffusion systems, and several others. Our hybrid model makes various assumptions (e.g., that a 2H V_{mem} profile would be stable, but HTHT would not be). We have put together a set of simulations to find viable parameter combinations that create worms meeting all these assumptions, thus ensuring that simulation results match experimental data. We tested a wide range of parameter combinations to find those that eventually satisfied all of the following requirements:

- WT and 2H worms are stable for electrodiffusion, but more complex patterns (e.g., HTHT) are not. This matches the data from Oviedo et al.³⁰ and numerous other observations, as well as being a part of our explanation for how Cryptic worms form.
- As we move the collision zone, the “electrodiffusion tail” (i.e., the location of the most hyperpolarized cell in the worm) moves with it. This validates our explanation of data in Bischof et al.⁴⁶
- Hyperpolarization turns all Cryptic worms into WT. This is from Durant et al.³⁴

- Hyperpolarization turns some 2H worms into WT; also from Durant et al.³⁴
- Depolarizing turns some WT worms into 2H.³³

The simulations are all done with BITSEY, which is a smaller version of the bioelectric-tissue simulator BETSE.⁴⁰ BITSEY is an open-source Python-based simulator that is available at <https://gitlab.com/grodstein/bitsey>. This publicly available repository contains not only the BITSEY source code but also the simulations supporting these experiments (in the worms/hybrid_model subdirectory). Note that BITSEY does not directly model axonal transport. Like BETSE, it models electrodiffusion. It has then been augmented to know the current direction of one or more VNCs, and to model the resulting head and tail pressure from the VNC(s) onto a worm's electrical state. The resulting electrodiffusion simulation then determines the simulated version of the worm's final V_{mem} pattern.

We specifically tested over 40,000 parameter combinations to find those that fit the requirements of the hybrid hypothesis. As opposed to Grodstein and Levin⁴² where we only needed to show which parameter sets could regenerate a substantial head-to-tail V_{mem} gradient, these new simulations also needed to show the extra conditions noted above, to guarantee that they predicted the experimental data. Simply setting the correct range of GJ size so that only the desired patterns can exist was by far the most stringent condition; only 555 parameter combinations met it. This is not surprising; Grodstein and Levin⁴² showed that electrodiffusion can only be robust if a system is in place to regulate GJ density (similar to the mammalian heart⁶⁹).

Of those 555 parameter combinations, we then tested the tightrope of cross-coupling strength. If the VNC pressures the electrodiffusion system too much, then Cryptic worms cannot exist (they would forever remain WT due to their still-WT VNC). If, however, there is too little pressure, then the meeting point of the two tails in a 2H worm cannot move the V_{mem} profile and we thus cannot explain the data from Figure 2. Several other data points from Durant et al.³⁴ also depend on the cross-coupling strength.

With these conditions, only 155 of the 555 (28%) parameter combinations were still successful. That is, there is an extra burden on planarian robustness, but it is not unreasonable.

Discussion

Planaria exhibiting divergent outcomes with respect to head number represent a fascinating aspect of collective emergent behavior. While a single worm may be stochastic at the organ level (having one or two heads), all the cells within that animal are in total agreement on what they are building—partial head/tail chimeras were not reported in any of the relevant experiments. Thus, we see a situation where the collective agent makes a stochastic choice, while all of the subunits (cells) must agree and cooperate toward the same goal.

This type of phenomenon is not unique to planaria. For example, inducers of carcinogenic conversion in tadpoles (a vertebrate model) that exhibit partial penetrance do so at the whole-animal level.^{70,71} In a cohort of animals, some percentage (e.g., 75%) may convert, while the remainder stay normal, in a stochastic manner. However, within a single animal, all the cells agree—the animal is either all

hyperpigmented or all normal. Understanding these phenomena shed light not only on specific examples of important biology relevant to regenerative medicine and cancer but also on the relationship between control systems operating at different levels of organization, and how they relate to each other within a multiscale living system.

Planaria are an important class of model species because they offer the possibility to study both highly robust outcomes and stochastic control, through a combination of genetic and epigenetic (in the original, broader sense of the word) instructive factors that set the target morphology toward which the cellular collective builds. Prior work offered several models addressing different aspects of the data, but had not been synthesized into a comprehensive understanding of various controls of regenerative outcomes. We have proposed a hybrid theory that relies on both electrodiffusion and axonal transport on an equal basis.

While each of those two hypotheses explains its own disjoint subset of the many planarian-regrowth experiments, the hybrid theory explains all of data that either of the two hypotheses does. It further explains Cryptic worms, which neither of the two hypotheses can easily explain. There are many existing planarian experiments. Some have interfered with TFs; others have interfered either with V_{mem} or with GJs; but none to our knowledge has interfered with both. We propose performing exactly these experiments. If they turn out as predicted, they should unambiguously support the hybrid hypothesis.

Why would evolution have resulted in two separate systems that feed into each other and into the final outcome? These questions are often difficult to answer, but we might speculate. Redundancy is a marvelous tool to achieve reliability. Planaria can regrow from small fragments after a predator attack; this rather expensive capability would only be cost efficient if it worked reliably. Axonal transport and electrodiffusion have complementary strengths and weaknesses:

- While planaria typically reproduce by fission, they are capable of sexual reproduction. Some system must be in place to establish a coordinate system before the VNC exists.
- As per Figure 1, electrodiffusion is quite robust to puncture wounds. Small (or even large) punctures that can easily disrupt VNC continuity make little difference in the overall V_{mem} profile from electrodiffusion.
- The VNC has the ability to utilize the resources of an intact brain to perform large-scale repatterning,⁴⁶ a far more sophisticated capability than electrodiffusion is capable of.

A similar situation seems to exist for the vertebrate limb, where the normal salamander limb is dependent on the nerve supply for regeneration, but limbs that develop in embryos without nerves can regenerate using some other signaling modality in its place.^{43,72} This suggests two parallel regeneration systems, one using neurons and one not. It is also possible that systems like this use a division of labor between the developmental toolkit genes supporting patterning modules,⁷³ and the ancient bioelectric system. The latter could be part of the biophysical toolkit serving a kind of memory to detect, store, and recall the morphologies produced by those modules.

The output of the bioelectric dynamics can feed back into these modules because in addition to redistributing morphogens, V_{mem} change can affect downstream pathways, including KRAS, Wnt, and Shh.^{74–78} Future work will test our predictions in planaria, as well as construct synthetic self-patterning systems using these principles to produce novel proto-organisms with useful functions.

Finally, there is substantial evidence of position-control genes being expressed in muscle fibers.⁴⁸ While the VNC hypothesis relies on neurons, it is interesting that the most prominent electrically excitable cells in planaria other than neurons are, of course, muscles. Muscles do not utilize axonal transport, and the use of muscles to express position-control genes is not universal across species.⁴⁸ Nonetheless, it would be interesting to look for more synergy here.

Acknowledgments

We thank Johanna Bischof, Fallon Durant, Chris Fields, and Alexis Pietak for helpful discussions about these topics. In addition, Johanna Bischof made extensive suggestions to greatly improve earlier drafts of this article.

Author Disclosure Statement

Both authors declare no conflict of interests.

Funding Information

We gratefully acknowledge support of The Guy Foundation and the John Templeton Foundation.

References

1. Davidson LA. Epithelial machines that shape the embryo. *Trends Cell Biol* 2012;22:82–87. DOI: 10.1016/j.tcb.2011.10.005.
2. Newman SA. Inherency and homomorphy in the evolution of development. *Curr Opin Genet Dev* 2019;57:1–8. DOI: 10.1016/j.gde.2019.05.006.
3. Harris MP. Bioelectric signaling as a unique regulator of development and regeneration. *Development* 2021;148. DOI: 10.1242/dev.180794.
4. Bates E. Ion channels in development and cancer. *Annu Rev Cell Dev Biol* 2015;31:231–247. DOI: 10.1146/annurev-cellbio-100814-125338.
5. Levin M. Bioelectric signaling: Reprogrammable circuits underlying embryogenesis, regeneration, and cancer. *Cell* 2021;184:1971–1989. DOI: 10.1016/j.cell.2021.02.034.
6. Owlarn S, Bartscherer K. Go ahead, grow a head! A planarian's guide to anterior regeneration. *Regeneration (Oxf)* 2016;3:139–155. DOI: 10.1002/reg.2.56.
7. Sheiman IM, Kreshchenko ND. Regeneration of planarians: Experimental object. *Russ J Dev Biol* 2015;46:1–9. DOI: 10.1134/S1062360415010075.
8. Lobo D, Beane WS, Levin M. Modeling planarian regeneration: A primer for reverse-engineering the worm. *PLoS Comput Biol* 2012;8:e1002481. DOI: 10.1371/journal.pcbi.1002481.
9. Saló E, Abril JF, Adell T, et al. Planarian regeneration: Achievements and future directions after 20 years of research. *Int J Dev Biol* 2009;53:1317–1327. DOI: 10.1387/ijdb.072414es.

10. Reddien PW. The cellular and molecular basis for planarian regeneration. *Cell* 2018;175:327–345. DOI: 10.1016/j.cell.2018.09.021.
11. Prindle A, Liu J, Asally M, et al. Ion channels enable electrical communication in bacterial communities. *Nature* 2015;527:59–63. DOI: 10.1038/nature15709.
12. Yang CY, Bialecka-Fornal M, Weatherwax C, et al. Encoding membrane-potential-based memory within a microbial community. *Cell Syst* 2020;10:417.e3–423.e3. DOI: 10.1016/j.cels.2020.04.002.
13. Levin M, Martyniuk CJ. The bioelectric code: An ancient computational medium for dynamic control of growth and form. *Biosystems* 2018;164:76–93. DOI: 10.1016/j.biosystems.2017.08.009.
14. Levin M, Pezzulo G, Finkelstein JM. Endogenous bioelectric signaling networks: Exploiting voltage gradients for control of growth and form. *Annu Rev Biomed Eng* 2017;19:353–387. DOI: 10.1146/annurev-bioeng-071114-040647.
15. Fields C, Bischof J, Levin M. Morphological coordination: A common ancestral function unifying neural and non-neural signaling. *Physiology (Bethesda)* 2020;35:16–30. DOI: 10.1152/physiol.00027.2019.
16. Levin M, Thorlin T, Robinson KR, et al. Asymmetries in H⁺/K⁺-ATPase and cell membrane potentials comprise a very early step in left-right patterning. *Cell* 2002;111:77–89.
17. Aw S, Koster J, Pearson W, et al. The ATP-sensitive K(+) channel (K(ATP)) controls early left-right patterning in *Xenopus* and chick embryos. *Dev Biol* 2010;346:39–53. DOI: 10.1016/j.ydbio.2010.07.011.
18. Morokuma J, Blackiston D, Levin M. KCNQ1 and KCNE1 K⁺ channel components are involved in early left-right patterning in *Xenopus laevis* embryos. *Cell Physiol Biochem* 2008;21:357–372.
19. Aw S, Adams DS, Qiu D, et al. H,K-ATPase protein localization and Kir4.1 function reveal concordance of three axes during early determination of left-right asymmetry. *Mech Dev* 2008;125:353–372.
20. Vandenberg LN, Morrie RD, Adams DS. V-ATPase-dependent ectodermal voltage and pH regionalization are required for craniofacial morphogenesis. *Dev Dyn* 2011;240:1889–1904. DOI: 10.1002/dvdy.22685.
21. Pai VP, Cervera J, Mafe S, et al. HCN2 channel-induced rescue of brain teratogenesis via local and long-range bioelectric repair. *Front Cell Neurosci* 2020;14. DOI: 10.3389/fncel.2020.00136.
22. Pai VP, Lemire JM, Pare JF, et al. Endogenous gradients of resting potential instructively pattern embryonic neural tissue via notch signaling and regulation of proliferation. *J Neurosci* 2015;35:4366–4385. DOI: 10.1523/JNEUROSCI.1877-14.2015.
23. Pai VP, Lemire JM, Chen Y, et al. Local and long-range endogenous resting potential gradients antagonistically regulate apoptosis and proliferation in the embryonic CNS. *Int J Dev Biol* 2015;59:327–340. DOI: 10.1387/ijdb.150197ml.
24. Chernet BT, Fields C, Levin M. Long-range gap junctional signaling controls oncogene-mediated tumorigenesis in *Xenopus laevis* embryos. *Front Physiol* 2015;5:519. DOI: 10.3389/fphys.2014.00519.
25. Chernet BT, Levin M. Transmembrane voltage potential of somatic cells controls oncogene-mediated tumorigenesis at long-range. *Oncotarget* 2014;5:3287–3306.
26. Chernet BT, Levin M. Transmembrane voltage potential is an essential cellular parameter for the detection and control of tumor development in a *Xenopus* model. *Dis Models Mech* 2013;6:595–607. DOI: 10.1242/dmm.010835.
27. Mathews J, Levin M. Gap junctional signaling in pattern regulation: Physiological network connectivity instructs growth and form. *Dev Neurobiol* 2017;77:643–673. DOI: 10.1002/dneu.22405.
28. Durant F, Lobo D, Hammelman J, et al. Physiological controls of large-scale patterning in planarian regeneration: A molecular and computational perspective on growth and form. *Regeneration (Oxf)* 2016;3:78–102. DOI: 10.1002/reg.2.54.
29. Levin M, Pietak AM, Bischof J. Planarian regeneration as a model of anatomical homeostasis: Recent progress in biophysical and computational approaches. *Semin Cell Dev Biol* 2018;87:125–144. DOI: 10.1016/j.semcdb.2018.04.003.
30. Oviedo NJ, Morokuma J, Walentek P, et al. Long-range neural and gap junction protein-mediated cues control polarity during planarian regeneration. *Dev Biol* 2010;339:188–199. DOI: 10.1016/j.ydbio.2009.12.012.
31. Nogi T, Levin M. Characterization of innexin gene expression and functional roles of gap-junctional communication in planarian regeneration. *Dev Biol* 2005;287:314–335.
32. Beane WS, Morokuma J, Adams DS, et al. A chemical genetics approach reveals H,K-ATPase-mediated membrane voltage is required for planarian head regeneration. *Chem Biol* 2011;18:77–89.
33. Durant F, Bischof J, Fields C, et al. The role of early bioelectric signals in the regeneration of planarian anterior/posterior polarity. *Biophys J* 2019;116:948–961. DOI: 10.1016/j.bpj.2019.01.029.
34. Durant F, Morokuma J, Fields C, et al. Long-term, stochastic editing of regenerative anatomy via targeting endogenous bioelectric gradients. *Biophys J* 2017;112:2231–2243. DOI: 10.1016/j.bpj.2017.04.011.
35. Dimmitt J, Marsh G. Electrical control of morphogenesis in regenerating *Dugesia tigrina*. II. Potential gradient vs. current density as control factors. *J Cell Comp Physiol* 1952;40:11–23. DOI: 10.1002/jcp.1030400103.
36. Marsh G, Beams HW. Electrical control of morphogenesis in regenerating *Dugesia tigrina*. I. Relation of axial polarity to field strength. *J Cell Comp Physiol* 1952;39:191–213. DOI: 10.1002/jcp.1030390203.
37. Lange CS, Steele VE. The mechanism of anterior-posterior polarity control in planarians. *Differentiation* 1978;11:1–12.
38. Palacios-Prado N, Bukauskas FF. Modulation of metabolic communication through gap junction channels by trans-junctional voltage; synergistic and antagonistic effects of gating and ionophoresis. *Biochim Biophys Acta* 2012;1818:1884–1894. DOI: 10.1016/j.bbamem.2011.09.001.
39. Pietak A, Levin M. Exploring instructive physiological signaling with the bioelectric tissue simulation engine. *Front Bioeng Biotechnol* 2016;4:55. DOI: 10.3389/fbioe.2016.00055.
40. Pietak A, Levin M. Bioelectric gene and reaction networks: Computational modelling of genetic, biochemical and bioelectrical dynamics in pattern regulation. *J R Soc Interface* 2017;14:20170425. DOI: 10.1098/rsif.2017.0425.
41. Nelson PC, Radosavljević M, Bromberg S. *Biological Physics: Energy, Information, Life*. New York: W.H. Freeman and Co., 2004: xxvi, 598.

42. Grodstein J, Levin M. Stability and Robustness Properties of Bioelectric Networks: A computational approach. *Bio-phys Rev* 2021;2:031305.
43. Singer M. A theory of the trophic nervous control of amphibian limb regeneration, including a re-evaluation of quantitative nerve requirements. In: Kiortsis V, Trampusch HAL, eds. *Regeneration in Animals and Related Problems*. Amsterdam: North Holland Publ. Co., 1965, pp. 20–32.
44. Kiortsis V, Trampusch HAL. *Regeneration in Animals and Related Problems*. Amsterdam: North-Holland Publisher, 1965.
45. Kiortsis V, Moraitou M. Factors of regeneration in *Spirographis spallanzanii*. In: Kiortsis V, Trampusch HAL, eds. *Regeneration in Animals and Related Problems*. Amsterdam: North Holland Publ. Co., 1965: 250–261.
46. Bischof J, Day ME, Miller KA, et al. Nervous system and tissue polarity dynamically adapt to new morphologies in planaria. *Dev Biol* 2020;467:51–65. DOI: 10.1016/j.ydbio.2020.08.009.
47. Pietak A, Bischof J, LaPalme J, et al. Neural control of body-plan axis in regenerating planaria. *PLoS Comput Biol* 2019;15:e1006904. DOI: 10.1371/journal.pcbi.1006904.
48. Reddien PW. Positional information and stem cells combine to result in planarian regeneration. *Cold Spring Harb Perspect Biol* 2021. DOI: 10.1101/cshperspect.a040717.
49. O'Brien J. Design principles of electrical synaptic plasticity. *Neurosci Lett* 2017;695:4–11. DOI: 10.1016/j.neulet.2017.09.003.
50. Miller AC, Pereda AE. The electrical synapse—Molecular complexities at the gap and beyond. *Dev Neurobiol* 2017; 77:562–574. DOI: 10.1002/dneu.22484.
51. Pereda AE, Curti S, Hoge G, et al. Gap junction-mediated electrical transmission: Regulatory mechanisms and plasticity. *Biochim Biophys Acta* 2013;1828:134–146. DOI: 10.1016/j.bbame.2012.05.026.
52. Pietak A, Levin M. Bioelectrical control of positional information in development and regeneration: A review of conceptual and computational advances. *Prog Biophys Mol Biol* 2018;137:52–68. DOI: 10.1016/j.pbiomolbio.2018.03.008.
53. Zhou J, Qin L, Tien JC, et al. Nkx3.1 functions as paratranscription factor to regulate gene expression and cell proliferation in non-cell autonomous manner. *J Biol Chem* 2012;287:17248–17256. DOI: 10.1074/jbc.M111.336909.
54. Lesaffre B, Joliot A, Prochiantz A, et al. Direct non-cell autonomous Pax6 activity regulates eye development in the zebrafish. *Neural Dev* 2007;22:2. DOI: 10.1186/1749-8104-2-2.
55. Vincent C, Gilabert-Juan J, Gibel-Russo R, et al. Non-cell-autonomous OTX2 transcription factor regulates anxiety-related behavior in the mouse. *Mol Psychiatry* 2021;26: 6469–6480. DOI: 10.1038/s41380-021-01132-y.
56. Torero Ibad R, Mazhar B, Vincent C, et al. OTX2 non-cell autonomous activity regulates inner retinal function. *eNeuro* 2020;7:1–11. DOI: 10.1523/ENEURO.0012–19.2020.
57. Planques A, Oliveira Moreira V, Dubreuil C, et al. OTX2 signals from the choroid plexus to regulate adult neurogenesis. *eNeuro* 2019;6:1–11. DOI: 10.1523/ENEURO.0262-18.2019.
58. Apulei J, Kim N, Testa D, et al. Non-cell autonomous OTX2 homeoprotein regulates visual cortex plasticity through Gadd45b/g. *Cereb Cortex* 2019;29:2384–2395. DOI: 10.1093/cercor/bhy108.
59. Bernard C, Vincent C, Testa D, et al. A mouse model for conditional secretion of specific single-chain antibodies provides genetic evidence for regulation of cortical plasticity by a non-cell autonomous homeoprotein transcription factor. *PLoS Genet* 2016;12:e1006035. DOI: 10.1371/journal.pgen.1006035.
60. Pastuzyn ED, Day CE, Kearns RB, et al. The neuronal gene arc encodes a repurposed retrotransposon gag protein that mediates intercellular RNA transfer. *Cell* 2018;172:275.e18–288.e18. DOI: 10.1016/j.cell.2017.12.024.
61. Ashley J, Cordy B, Lucia D, et al. Retrovirus-like Gag protein Arc1 binds RNA and traffics across synaptic boutons. *Cell* 2018;172:262.e11–274.e11. DOI: 10.1016/j.cell.2017.12.022.
62. Oviedo NJ, Nicolas CL, Adams DS, et al. Live imaging of planarian membrane potential using DiBAC4(3). *CSH Protoc* 2008;2008:pdb.prot5055.
63. Adams DS, Levin M. Measuring resting membrane potential using the fluorescent voltage reporters DiBAC4(3) and CC2-DMPE. *Cold Spring Harbor protocols* 2012;2012: 459–464. DOI: 10.1101/pdb.prot067702.
64. Emmons-Bell M, Durant F, Hammelman J, et al. Gap junctional blockade stochastically induces different species-specific head anatomies in genetically wild-type *Girardia dorocephala* flatworms. *Int J Mol Sci* 2015;16:27865–27896. DOI: 10.3390/ijms161126065.
65. Adler EL, Woodruff RI. Varied effects of 1-octanol on gap junctional communication between ovarian epithelial cells and oocytes of *Oncopeltus fasciatus*, *Hyalophora cecropia*, and *Drosophila melanogaster*. *Arch Insect Biochem Physiol* 2000;43:22–32.
66. Pappas CA, Rioult MG, Ransom BR. Octanol, a gap junction uncoupling agent, changes intracellular [H⁺] in rat astrocytes. *Glia* 1996;16:7–15.
67. McAdams HH, Arkin A. It's a noisy business! Genetic regulation at the nanomolar scale. *Trends Genet* 1999;15: 65–69.
68. Vu HT, Mansour S, Kucken M, et al. Dynamic polarization of the multiciliated planarian epidermis between body plan landmarks. *Dev Cell* 2019;51:526.e6–542.e6. DOI: 10.1016/j.devcel.2019.10.022.
69. Kleber AG, Jin Q. Coupling between cardiac cells—An important determinant of electrical impulse propagation and arrhythmogenesis. *Biophys Rev* 2021;2:031301. DOI: 10.1063/5.0050192.
70. Lobo D, Lobikin M, Levin M. Discovering novel phenotypes with automatically inferred dynamic models: A partial melanocyte conversion in *Xenopus*. *Sci Rep* 2017;7: 41339. DOI: 10.1038/srep41339.
71. Lobikin M, Lobo D, Blackiston DJ, et al. Serotonergic regulation of melanocyte conversion: A bioelectrically regulated network for stochastic all-or-none hyperpigmentation. *Sci Signal* 2015;8:ra99. DOI: 10.1126/scisignal.aac6609.
72. Yntema CL. Regeneration in sparsely innervated and aneurogenic forelimbs of *Amblystoma* larvae. *J Exp Zool* 1959;140:101–123.
73. Newman SA, Bhat R. Dynamical patterning modules: A “pattern language” for development and evolution of multicellular form. *The International journal of developmental biology* 2009;53:693–705. DOI: 10.1387/ijdb.072481sn.

74. Borodinsky LN, Belgacem YH, Swapna I, et al. Spatio-temporal integration of developmental cues in neural development. *Dev Neurobiol* 2015;75:349–359. DOI: 10.1002/dneu.22254.
75. Belgacem YH, Borodinsky LN. Inversion of Sonic hedgehog action on its canonical pathway by electrical activity. *Proc Natl Acad Sci U S A* 2015;112:4140–4145. DOI: 10.1073/pnas.1419690112.
76. Atsuta Y, Tomizawa RR, Levin M, et al. L-type voltage-gated Ca^{2+} channel CaV1.2 regulates chondrogenesis during limb development. *Proc Natl Acad Sci U S A* 2019; 116:21592–21601. DOI: 10.1073/pnas.1908981116.
77. McLaughlin KA, Levin M. Bioelectric signaling in regeneration: Mechanisms of ionic controls of growth and form. *Dev Biol* 2018;433:177–189. DOI: 10.1016/j.ydbio.2017.08.032.
78. Zhou Y, Wong CO, Cho KJ, et al. Signal transduction. Membrane potential modulates plasma membrane phospholipid dynamics and K-Ras signaling. *Science* 2015;349: 873–876. DOI: 10.1126/science.aaa5619.

Address correspondence to:

Michael Levin, PhD

Allen Discovery Center at Tufts University

200 College Avenue

Medford, MA 02155

USA

E-mail: michael.levin@tufts.edu